

## Dynamic Light Scattering Study of the Inhibiting Effect on Crystal Growth of Calcium Carbonate

Natsumi Kamiya,<sup>\*1</sup> Fumiaki Tsunomori,<sup>2</sup> Hiroyuki Kagi,<sup>2</sup> and Kenji Notsu<sup>2</sup>

<sup>1</sup>Department of Applied Chemistry, National Defense Academy, Yokosuka, Kanagawa 239-0811

<sup>2</sup>Geochemical Research Center, Graduate School of Science, The University of Tokyo, Bunkyo-ku, Tokyo 113-0033

Received August 19, 2010; E-mail: natsumi@nda.ac.jp

This study reports the first application of dynamic light scattering to observations of crystal growth of calcium carbonate from a supersaturated solution. Crystal size distributions around the critical nucleus radius ( $\approx 2$  nm at  $\Omega = 18$ ) were measured in La-free and 5  $\mu$ M La-doped conditions. In the former, the intensity of scattered light increased smoothly and particle size increased with time. In the case of La-doped condition, the total scattering volume of particles was smaller, and grew very slowly compared with the La-free condition. These results show that the inhibiting effect of  $\text{La}^{3+}$  on calcium carbonate occurred from the initial stage of crystal growth.

Calcium carbonates play an important role in the global carbon cycle, because both crystallization and dissolution of calcium carbonates occur in marine environments, thereby controlling the atmospheric  $\text{CO}_2$  content which is closely related to global warming.<sup>1</sup> The nucleation and crystal growth of calcium carbonates are also familiar phenomena, for example, biomineralization or scale precipitation in geothermal areas. It has therefore been critical to obtain knowledge of crystallization and dissolution of calcium carbonate. Consequently, a number of studies have been reported on the precipitation and crystal growth of calcium carbonate in supersaturated solutions.<sup>2–4</sup>

A supersaturated solution of calcium carbonate without any additives produces initially a metastable phase, which is then transformed into a more stable phase according to the Ostwald step rule.<sup>5,6</sup> Calcite is the most stable phase in ambient conditions, while aragonite and vaterite are metastable phases under these conditions.<sup>7,8</sup> These polymorphs are also known to be stabilized by impurities.<sup>9–12</sup> Among these, lanthanum ion ( $\text{La}^{3+}$ ) has been reported to be an effective additive for stabilizing metastable phases of calcium carbonate. The inhibiting effect of  $\text{La}^{3+}$  on the formation of calcite was first reported by Akagi and Kono.<sup>13</sup> Tsuno et al.<sup>14</sup> reported that the addition of approximately 10  $\mu$ M  $\text{La}^{3+}$  into a supersaturated solution of calcium carbonate yielded stabilization of vaterite. As a possible explanation of this phenomenon, Kamiya et al.<sup>15</sup> suggested that  $\text{La}^{3+}$  exclusively inhibits crystal growth of calcite. However, the inhibition mechanism has not been clear, and it is needed to find how the  $\text{La}^{3+}$  inhibitor affects calcium carbonate precipitation and crystal growth.

In a number of previous studies, microscopic observations using scanning electron microscopy (SEM) and atomic force microscopy (AFM) have been adopted for observations of crystal growth. However, these methods cannot be used to observe the size of a critical nucleus for calcium carbonate (about a few nanometers).<sup>16</sup> In addition, in situ observations of nanometer-size particles in a solution are necessary to inves-

tigate detailed kinetic processes of precipitation and crystal growth. In this study therefore, we adopted dynamic light scattering (DLS) to measure time evolution of the particle size distribution of calcium carbonate. The size distribution in the initial stages of crystal growth of calcium carbonate and the impurity effects of  $\text{La}^{3+}$  on crystal growth of calcium carbonate are discussed on the basis of DLS measurements and SEM observations.

### Experimental

**Dynamic Light Scattering (DLS) Apparatus.** In the initial stage of the crystal growth of calcium carbonate after mixing sodium hydrogen carbonate ( $\text{NaHCO}_3$ ) and calcium chloride ( $\text{CaCl}_2$ ) solutions, the concentration of calcium carbonate particles in the system will be quite low. To obtain good data from this sample, a highly sensitive detector of scattered light is required. We therefore adopted an avalanche photodiode (High Q.E. APD, ALV Co., Ltd.) because quantum yield is quite high ( $>80\%$  at 632.8 nm). In order to use the avalanche photodiode, we assembled a dynamic light scattering apparatus. A 632.8-nm line of a He-Ne laser (18 mW) was used as the incident beam. An autocorrelation function of the scattered light was obtained with a correlator (Flex99R-12, Correlator.com). The angle between the incident beam and the detector was  $30^\circ$ . A 50-mm by 10-mm NMR tube was used as the sample cell to preventing distortion of the incident beam and the scattered light. Two pinholes with a diameter of 150  $\mu$ m were set behind the cell and in front of the detector. Previous studies have successfully applied DLS to the crystal growth of hydroxyapatite<sup>17</sup> and zeolite.<sup>18</sup> The obtained crystal growth rate of hydroxyapatite was several orders of magnitude lower than that of other inorganic crystals under the same supersaturated condition.<sup>19</sup> DLS data of zeolite were obtained at ordinary temperature and pressure where crystal growth of zeolite does not occur. Consequently, the particle size stays constant during measurement. On the other hand, in this study, particle size distribution can change while measuring because nucleation

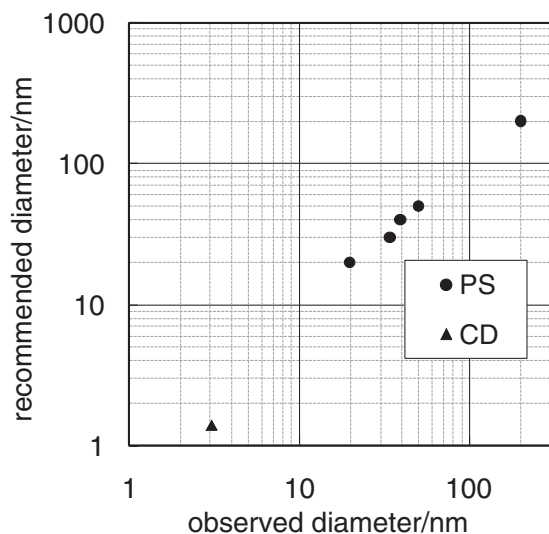


**Figure 1.** Plots of the calibration measurements. Polystyrene particles (PS) with diameters of 20, 30, 40, 50, and 200 nm, and a 1.5 nm cyclodextrin molecule (CD) were used as standard samples.

and crystal growth occur continuously and a broad distribution of particle sizes are expected under these conditions (See sample preparation). In addition, the crystal growth of calcium carbonate is expected to be unimodal. Therefore we adopted a histogram for analyzing all autocorrelation functions in this study. The total number of histogram bins used in the analysis was 55. Correlation times corresponding to each decay rate were estimated by a nonlinear least-squares method. Then the mean diameter of particles in the solution was calculated on the basis of DLS theory.<sup>20</sup> In this study, the intermolecular interaction on evaluated hydrodynamic radius of a particle among each experimental condition was not taken into account, because our attention was focused on the relative change of the apparent hydrodynamic radius. Accuracy confirmation of the apparatus was carried out using polystyrene particles (Duke Scientific Co.) whose diameters were 20, 30, 40, 50, and 200 nm, and cyclodextrin whose molecular diameter was about 1.4 nm (Sigma-Aldrich Co.). The results of the calibration are shown in Figure 1. The diameters of particles obtained from the present instrument corresponded with the recommended diameters.

**Sample Preparation.** The supersaturation state of a solution with respect to calcite,  $\Omega_{\text{cal}}$ , is defined as

$$\Omega_{\text{cal}} = a_{\text{Ca}^{2+}} \cdot a_{\text{CO}_3^{2-}} / K_{\text{sp}}(\text{calcite}) \quad (1)$$

where  $a_{\text{Ca}^{2+}}$  and  $a_{\text{CO}_3^{2-}}$  are the activities of calcium ions and carbonate ions, respectively.  $K_{\text{sp}}$  is the solubility product constant of calcite. The supersaturated solution of calcium carbonate was prepared by dissolving analytical-grade reagents (Wako Co.) with Milli-Q water. The composition of the solution was as follows; 1.40 mM  $\text{NaHCO}_3$  solution, the pH of which was controlled at 10.8 by the addition of a sodium hydroxide (NaOH) solution, and 0.225 mM  $\text{CaCl}_2$  solution were prepared respectively. The two solutions were treated with a syringe filter whose pore diameter is 200 nm, mixed in a Teflon vessel. This mixture (pH 10.5) was then stirred in an

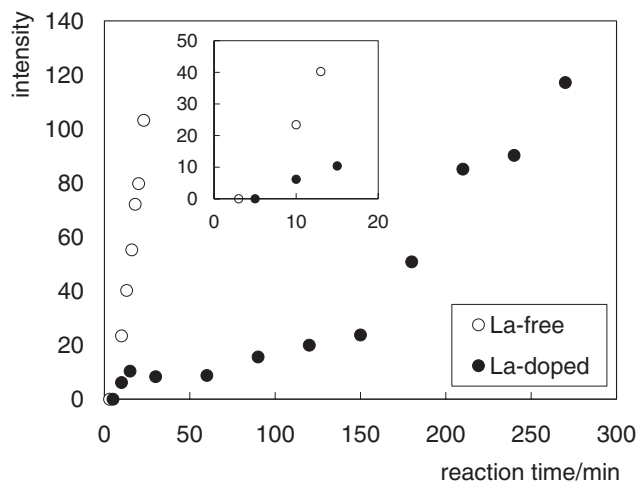


**Figure 2.** Plots of the cumulative intensity vs. reaction time. The upper-limit was about 100 to avoid the multiple scattering effect.

open system and subsequently, neither the addition of other solution nor pH control were carried out. About 3 mL of the mixed solution was collected at a certain period of time and this solution was injected into the DLS sample cell; each measurement took 10 s. In this experiment,  $\Omega_{\text{cal}}$  of the solution was set to about 18, as calculated by visual MINTEQ ver. 2.51. For the La-doped experiment, lanthanum chloride ( $\text{LaCl}_3$ ) was added into the  $\text{CaCl}_2$  solution before starting the reaction. The concentration of  $\text{La}^{3+}$  was adjusted to 5  $\mu\text{M}$  in the supersaturated solution.

**SEM Observation and Phase Identification of Crystallized Particles.** The samples were collected by filtration (hydrophilic PTFE membrane filter, pore size: 100 nm) at 25 min from the beginning of the reaction in the La-free solution, and at 350 min in the La-doped solution. The La-doped measurement took longer than the La-free experiment as we discuss later. The filtered samples were dried at 110  $^{\circ}\text{C}$  in air for 24 h. The samples of calcium carbonate thus obtained were examined using a VE-9800 Scanning Electron Microscope (KEYENCE Co.). The samples were coated with gold to avoid charging in the SEM and secondary electron images were obtained with an acceleration voltage of 10 kV. Powder X-ray diffraction measurements were carried out using a Gandolfi camera (114-mm diameter) with the  $\text{Cu K}\alpha$  line.

## Results and Discussion

**DLS Measurement.** Figure 2 shows plots of the cumulative value of the obtained  $g^2(\tau)$  as a function of the reaction time. The cumulative value of the second-order autocorrelation curve corresponds to the total scattering volume of particles in the sample solution. In other words, the increase in the cumulative intensity corresponds to the increase in particle number and particle size. The data that are shown as zero in intensity were below the detection limit, which occurs when the fitting cannot be conducted to the correlation function because of weak scattered light. In the La-free experiment, the cumulative intensity (arbitrary unit) increased gradually with time until the intensity approached about 100 in 23 min. In our experiment, the sample, whose cumulative intensity was over

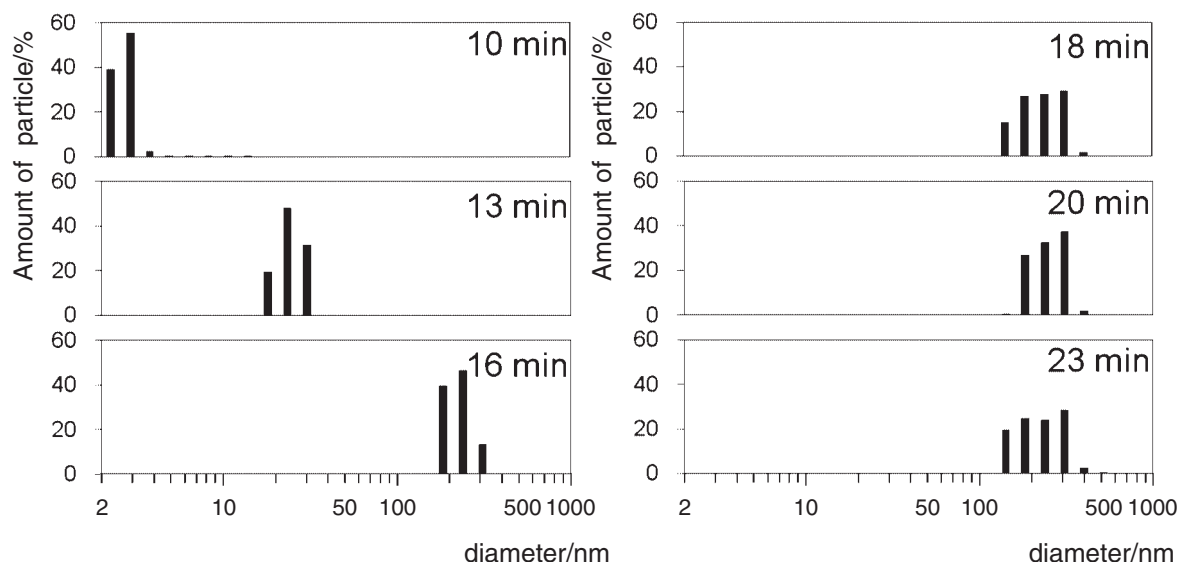


**Figure 3.** Particle size distribution in the La-free experiment based on DLS measurements.

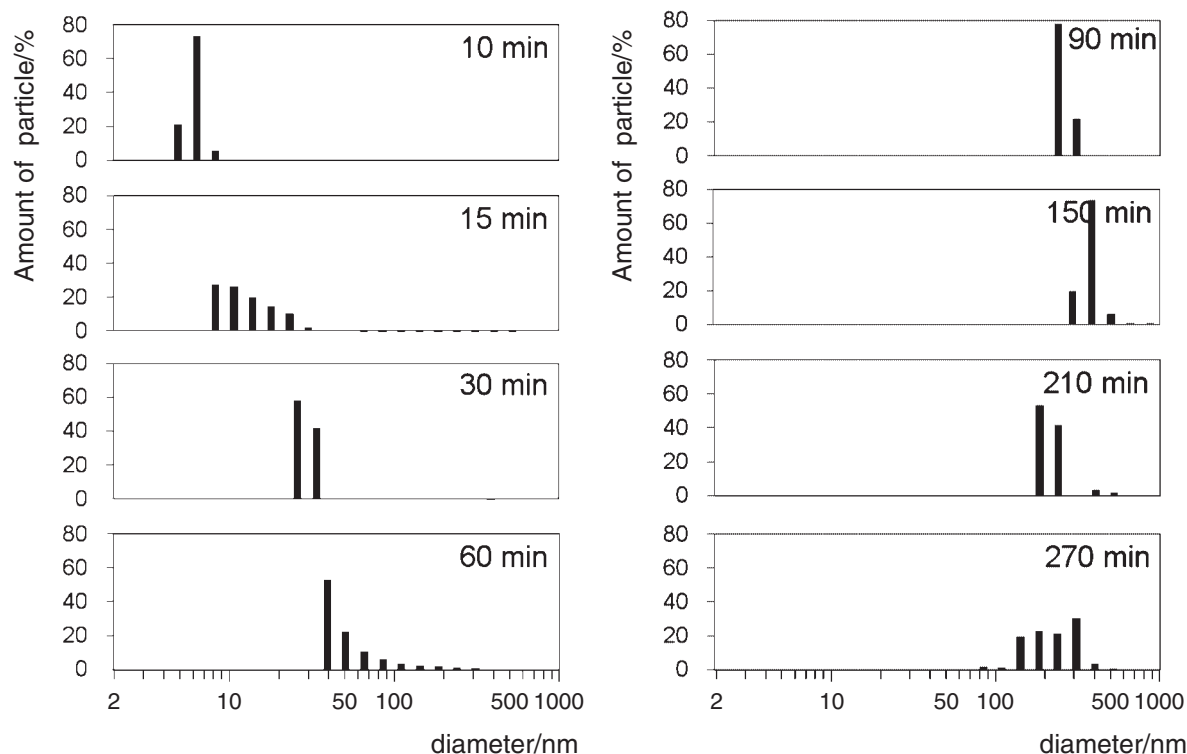
100, could not provide a correct correlation curve because of the multiple scattering effect.<sup>21</sup> On the other hand, under the La-doped condition, more reaction time (270 min) was needed for the cumulative intensity to exceed 100. These results clearly show that  $\text{La}^{3+}$  inhibits precipitation and crystal growth of calcium carbonate. In both the La-free and La-doped conditions, no decay of the second-order autocorrelation curve was observed at 5 min from the start of the reaction. This suggests that there were no detectable particles in the solution. At 10 min from the beginning of the reaction, the cumulative intensity was more than 23 under the La-free condition. On the other hand, in the La-doped condition, the intensity was about 6, which was only a quarter the value of the La-free condition. This suggests that under the La-doped condition, the amount of particle precipitation was remarkably less than that under the La-free condition in the initial stages of crystal growth.

Particle size distributions obtained from DLS measurements under the La-free condition are presented in Figure 3. Particle size distribution was number weighting. The amounts of particle are presented as the percentage of the corresponding size in the total number. The effect of gravity is more dominant than the diffusion of particles when the particle size is larger than  $1\ \mu\text{m}$  in solution;<sup>22</sup> the upper detection limit is  $1\ \mu\text{m}$  in the DLS apparatus. For this reason, the histograms thus show a range of particle sizes from 2 nm to  $1\ \mu\text{m}$ . At 10 min from the start of the reaction, a distribution peak at about 2.5 nm was observed; this size is comparable to the size of the critical nucleus of calcium carbonate at  $\Omega = 18$  ( $\approx 2\ \text{nm}$ ) estimated from the change in the Gibbs free energy.<sup>16</sup> This value also corresponds to the sizes of stable prenucleation ion clusters (the nucleation clusters and their aggregates are 0.6–1.1 and 2–4 nm in size, respectively).<sup>23</sup> This coincidence suggests that the particle size distribution of the critical nucleus of calcium carbonate was successfully detected by DLS. The size distribution shifted toward larger particle sizes up to 18 min, and then remained unchanged. On the other hand, Figure 2 shows that the cumulative intensity increased even after 18 min, and therefore the total scattering volume of the particles should increase.

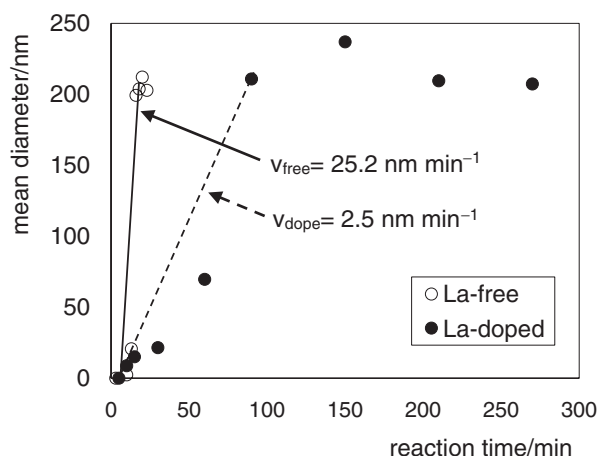
The results of the experiments in the La-doped condition are shown in Figure 4. A particle size distribution was observed at about 8.5 nm at 10 min after the start of the reaction. In this case, the shift in the distribution was much slower than for the La-free condition. The average particle size grew to 200 nm in 90 min, 5 times slower than for the La-free condition, and their sizes then remained constant until the end of the measurement (270 min). Figure 2 indicates that the cumulative intensity increased after 90 min. This implies that only the total scattering volume of the particles increased, whereas the particle size was unchanged. In other words, the number of particles increased while the particle size stayed constant after 90 min.

Figure 5 shows plots of the mean diameter obtained from both experiments as a function of the reaction time. For both conditions, particle sizes increased up to 200 nm and then remained constant. The crystal growth rate,  $v$ , was estimated by a linear approximation of the particle growth up to 200 nm. The growth rate of the particles in the La-free condition,  $v_{\text{free}}$ , was calculated to be  $25.2\ \text{nm min}^{-1}$ , and that in the La-doped condition,  $v_{\text{dope}}$ , was  $2.5\ \text{nm min}^{-1}$ . The addition of  $\text{La}^{3+}$  thus substantially decreased the growth rate of the particles ( $v_{\text{dope}}/v_{\text{free}} = 0.1$ ). For example, aspartic acid, which has been reported to be an effective impurity for retarding crystal growth and dissolution of calcite, requires a concentration of more than 0.15 M to reach  $v_{\text{dope}}/v_{\text{free}} = 0.1$ .<sup>24</sup> In the case of the addition of 4 mM of  $\text{Ba}^{2+}$ , the value of  $v_{\text{dope}}/v_{\text{free}}$  also only decreased to 0.56.<sup>25</sup> The effect of  $\text{La}^{3+}$  on crystal growth of calcium carbonate is thus more effective than the other additives mentioned above.

**SEM Observations and XRD Characterization.** The DLS experiments showed that particles of about 200 nm remained until the end of the measurement. The SEM study was carried out to confirm the particle size distribution obtained using the DLS method. Figure 6 shows SEM images of the suspended particles which were collected at 25 and 350 min, under La-free and La-doped conditions, respectively. In the La-free experiment, two different morphologies were observed,



**Figure 4.** Particle size distribution in the La-doped experiment based on DLS measurements.



**Figure 5.** Plots of the mean diameter at each reaction time.

The solid line indicates the crystal growth rate in the La-free condition ( $v_{\text{free}}$ ) and the dashed line indicates the growth rate in the La-doped condition ( $v_{\text{dope}}$ ).

rice-shaped particles about 200–500 nm and hexagonal disk-shaped particles about 1–2  $\mu\text{m}$  in size (Figure 6a). In this experiment, the degree of supersaturation decreased continuously with progress of reaction because pH control and addition of other solutions were not carried out in the course of the reaction. At the start of the reaction, nucleation occurred and crystal growth proceeded because of the high degree of supersaturation. The initial precipitates grew steadily and sized up to beyond 1  $\mu\text{m}$ . These crystals cannot be detected by the DLS measurement. In contrast, the crystals which were generated after the degree of supersaturation decreased grew slower than the former did. These two kinds of crystals

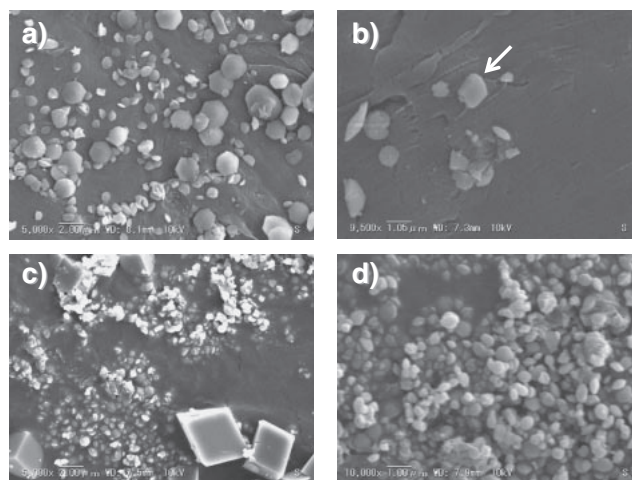


**Figure 6.** SEM images of the samples obtained (a, b) in the La-free experiment after 25 min from the start, and (c, d) in the La-doped experiment after 350 min from the start. The scale bar is (a, c) 2  $\mu\text{m}$  and (b, d) 1  $\mu\text{m}$ . The rhombohedral-like crystal is shown by an arrow in (b).

correspond to hexagonal particles and rice-shaped particles shown in Figures 6a and 6b, respectively. The obtained particle sizes in the SEM observations agree with the DLS data (Figure 3) except for the 1–2  $\mu\text{m}$  particles. The upper limit in the particle size detected with DLS in the instrument used in this study is 1  $\mu\text{m}$  as mentioned already. Diffraction lines corresponding to vaterite and the strongest line of calcite (104) were found in the XRD patterns (data not shown). The morphology of some of the larger particles was rhombohedral-like (Figure 6b). This morphology is similar to those reported

for crystals in the transformation from vaterite to calcite in a previous study.<sup>6</sup> The disk-shaped particles observed in this study may correspond to calcite transforming from vaterite.

For the La-doped condition as well,  $\approx 200\text{--}500\text{ nm}$  particles and calcite crystals (rhombohedral) with particle sizes larger than  $1\text{ }\mu\text{m}$  were observed. The former particle sizes also agree with the DLS results shown in Figure 4. Diffraction lines of calcite  $\{(104), (113), (202), (018), (116), (214)\}$  were observed from this sample. These results suggested that the small particles were retained, even though some particles grew to more than  $1\text{ }\mu\text{m}$ . The crystals were thus transformed from vaterite to calcite, and then some of the calcite grew larger while others remained smaller than  $1\text{ }\mu\text{m}$ . The morphology of these small particles was not rhombohedral; however, lanthanum compounds were not detected by XRD. Kamiya et al. have reported that lanthanum carbonate precipitated on the step sites of calcite and lanthanum carbonate does not form epitaxially on the calcite surface.<sup>15</sup> The reason that two kinds of crystals appeared is the same of the La-free experiment. No effects of  $\text{La}^{3+}$  were observed for the larger crystals because the growth of these crystals is fast due to the high degree of supersaturation. In contrast, for the smaller crystals, the inhibition effects of  $\text{La}^{3+}$  on the crystal surface appeared, because these crystals grew slowly due to the low degree of supersaturation. However, lanthanum compounds could not be detected by XRD because their amounts were much smaller than calcium carbonate or those compounds had no periodic structure.

Gebauer et al. have reported that ACC II (amorphous calcium carbonate II) precipitates at higher pH and then transforms to vaterite.<sup>23</sup> However, in our experiments, the mixed solution of pH was 10.5 that is higher than that reported by Gebauer et al. and vaterite was also detected in the La-free condition by XRD. The experimental conditions of Gebauer et al. were different from ours in the control of solution composition and pH and these results cannot be compared directly. As the secondary smaller particles were exclusively affected by  $\text{La}^{3+}$  (no effect for the primary larger particles), it is suggested that the adsorption rate of  $\text{La}^{3+}$  on the crystal surface competed with the crystal growth rate of calcium carbonate. This suggests that the inhibition effect of  $\text{La}^{3+}$  appeared in the crystal growth of vaterite. This study demonstrated that the presence of  $\text{La}^{3+}$  in the supersaturated solution affects drastically the nucleation and accumulation of particles of calcium carbonate.

### Conclusion

The nucleation and crystal growth process of calcium carbonate were progressively monitored using DLS. The particle size distribution of the critical nucleus of calcium carbonate was detected. Under the La-free condition, the particle sizes increased at a rate of  $25.2\text{ nm min}^{-1}$  until reaching about  $200\text{--}500\text{ nm}$ . The larger particles transformed from vaterite to calcite 25 min after the start of the reaction. In contrast, under the  $5\text{ }\mu\text{M}$  La-doped condition, the particles sizes increased  $2.5\text{ nm min}^{-1}$  and it took 10 times longer to produce particles of  $200\text{--}500\text{ nm}$  than in the La-free condition. These

observations show that there is an inhibiting effect of  $\text{La}^{3+}$  on the initial stage of crystal growth of calcium carbonate.

The authors are grateful to Prof. Hiroshi Tsuno (Fac. of Education and Human Sciences, Yokohama National University) for technical assistance in performing the XRD measurements; Mr. Naoki Okumura (KEYENCE Co.) for his assistance with the SEM observations.

### Supporting Information

Correlation function at 10 min after starting reaction in La-free condition. This material is available free of charge on the web at <http://www.csj.jp/journals/bcsj/>.

### References

- 1 A. Ridgwell, R. E. Zeebe, *Earth Planet. Sci. Lett.* **2005**, *234*, 299.
- 2 L. N. Plummer, E. Busenberg, *Geochim. Cosmochim. Acta* **1982**, *46*, 1011.
- 3 O. Söhnel, J. W. Mullin, *J. Cryst. Growth* **1982**, *60*, 239.
- 4 S. R. Dickinson, G. E. Henderson, K. M. McGrath, *J. Cryst. Growth* **2002**, *244*, 369.
- 5 T. Ogino, T. Suzuki, K. Sawada, *Geochim. Cosmochim. Acta* **1987**, *51*, 2757.
- 6 N. Spanos, P. G. Koutsoukos, *J. Cryst. Growth* **1998**, *191*, 783.
- 7 H. J. Meyer, *Z. Kristallogr.* **1965**, *121*, 220.
- 8 D. Kralj, L. Brečević, A. E. Nielsen, *J. Cryst. Growth* **1990**, *104*, 793.
- 9 Y. Kitano, D. W. Hood, *Geochim. Cosmochim. Acta* **1965**, *29*, 29.
- 10 J. Kanakis, E. Dalas, *J. Cryst. Growth* **2000**, *219*, 277.
- 11 A. Kai, T. Miki, *Jpn. J. Appl. Phys.* **2000**, *39*, L1071.
- 12 F. Manoli, E. Dalas, *J. Cryst. Growth* **2001**, *222*, 293.
- 13 T. Akagi, Y. Kono, *Aquat. Geochem.* **1995**, *1*, 231.
- 14 H. Tsuno, H. Kagi, T. Akagi, *Bull. Chem. Soc. Jpn.* **2001**, *74*, 479.
- 15 N. Kamiya, H. Kagi, F. Tsunomori, H. Tsuno, K. Notsu, *J. Cryst. Growth* **2004**, *267*, 635.
- 16 J. W. Morse, R. S. Arvidson, A. Lüttge, *Chem. Rev.* **2007**, *107*, 342.
- 17 K. Onuma, A. Ito, *Chem. Mater.* **1998**, *10*, 3346.
- 18 S. Mintova, V. Valtchev, *Microporous Mesoporous Mater.* **2002**, *55*, 171.
- 19 K. Onuma, A. Ito, T. Tateishi, *J. Cryst. Growth* **1996**, *167*, 773.
- 20 J. B. Berne, R. Pecora, *Dynamic Light Scattering: With Applications to Chemistry, Biology, and Physics*, Dover Publications, Inc., New York, **2000**.
- 21 G. Mie, *Ann. Phys.* **1908**, *330*, 377.
- 22 G. G. Stokes, *Trans. Cambridge Philos. Soc.* **1851**, *9*, 8.
- 23 D. Gebauer, A. Völkel, H. Cölfen, *Science* **2008**, *322*, 1819.
- 24 S. Elhadj, J. J. De Yoreo, J. R. Hoyer, P. M. Dove, *Proc. Natl. Acad. Sci. U.S.A.* **2006**, *103*, 19237.
- 25 J. M. Astilleros, C. M. Pina, L. Fernández-Díaz, A. Putnis, *Geochim. Cosmochim. Acta* **2000**, *64*, 2965.